High Current Turn-off of GaN HEMT for Solid-state Circuit Breaker at Cryogenic Temperatures

Zhou Dong
ABB US Research Center
ABB. Inc
Raleigh, USA
zhou.dong@us.abb.com

Ching-Hsiang Yang
CURENT
University of Tennessee
Knoxville, USA
cyang30@vols.utk.edu

Shimul K. Dam
CURENT
University of Tennessee
Knoxville, USA
sdam@utk.edu

Dehao Qin
Clemson University
North Charleston, USA
dehaoq@g.clemson.edu

Ruirui Chen
CURENT
University of Tennessee
Knoxville, USA
rchen14@vols.utk.edu

Fred (Fei) Wang
CURENT
University of Tennessee
Oak Ridge National Laboratory
Knoxville, USA
fred.wang@utk.edu

Hua Bai
CURENT
University of Tennessee
Knoxville, USA
hbai2@utk.edu

Zheyu Zhang
Clemson University
North Charleston, USA
zheyuz@clemson.edu

***Abstract*— Gallium Nitride (GaN) high electron mobility transistors (HEMTs) are superior for cryogenically cooled solid-state circuit breakers (SSCBs) in future aircraft applications owing to their low on-resistance and high saturation current. However, during the high current turn-off, it is found that potential voltage and current ringing could happen to damage the device. In this paper, the turn-off failure mechanism of 650V/150A GaN bare dies are analyzed, which could be due to the instability of paralleled switching cells in one GaN bare die. A solution is proposed to use an RC snubber to reduce the overlap of v_{ds} and i_d in the turn-off process to avoid the unstable region where the hard-switching trajectory goes through. Experiments are conducted to verify the effectiveness of the proposed solution. With the reduced overlap between v_{ds} and i_d, the GaN HEMT successfully turns off the 550 A objective current.**

Keywords—GaN HEMT, Cryogenic power electronics, solid-state circuit breaker, electrified aircraft

I. INTRODUCTION

Electrified aircraft propulsion (EAP) can improve fuel efficiency and reduce CO_2 emission compared to conventional engines [1]. The noise levels can also be dramatically reduced in commercial transport aircrafts so that the airports can be built in densely populated areas to benefit economy [2]. Superconducting techniques could be potentially applied in the future EAP to reduce the loss and weight of cables, motors, power electronics equipment, etc [3]. Cryogenic cooling (<-153°C) is a key enabler, which could utilize liquid hydrogen as the coolant for system components [4]. After cooling the system components, the hydrogen warms up and would be ready to be used as the fuel for propulsion.

On the other hand, the potential dc distribution could be adopted for overall higher efficiency in the EAP. With the dc distribution, the solid-state circuit breaker (SSCB) is attractive because of the fast protection speed to shut down the high fault current without a zero-crossing point. However, the high conduction loss of the SSCB and the corresponding heavy thermal management system are the main concerns. Luckily, cryogenic cooling is the potential to dramatically reduce the conduction loss while keeping other benefits of the SSCB.

The gallium nitride (GaN) high electron mobility transistor (HEMT) features a much smaller on-resistance at cryogenic temperature compared to the room temperature condition [5]. Therefore, applying the GaN HEMT as the main switch of the SSCB is very attractive for cryogenic applications. Moreover, the higher saturation current level at cryogenic temperatures enables a higher let-through fault current. This is important because SSCB normally requires a much higher let-through current compared to the rated current (5~10 times) to avoid nuisance trips [6]. However, the destructive ringing is observed by researchers during high current switching process. For example, in [7], the device failed at high-current turn-off transient. The mechanism is still not well explained, and solutions are very limited. Such high-current turn-off capability is significant in SSCB applications for reliable protection purposes.

In this paper, the device failure is observed when a GaN bare die (650 V and ~150 A rated) turns off ~480 A at -180°C. The mechanism of the failure is analyzed. Moreover, it is found that with smaller voltage and current overlap during turn-off, the device can survive at a higher turn-off current. This characteristic can potentially help GaN-based SSCBs fully utilize the device capability.

The remainder of this paper is organized as follows. Section II introduces the basic operating principal of the SSCB and the advantage of using GaN HEMTs as the main switch in SSCBs. Section III describes the device failure at high current turn-off applications and analyzes the possible failure mechanism. Section IV introduces the proposed solution for higher turn-off current capability and verifies the analysis and the proposed solution with simulation and experimental results. Section V concludes the paper.

II. Utilizing GaN HEMTs in Cryogenic Cooled SSCB Applications

A. SSCB Basic Working Principle

Fig. 1 shows an example of a SSCB in a dc system. The semiconductor switch S_1 is used to open and close the SSCB. The voltage clamping unit T_1, which could be the metal oxide varistor (MOV), the transient voltage suppressor (TVS) diode, or others, is used to clamp the device voltage during the turn-off of S_1 and absorb the inductive energy after turning off S_1. For example, with a TVS diode adopted in Fig. 1, after S_1 turns off, the fault current through L_s would flow through T_1 to break down the TVS diode. The clamping voltage of the TVS diode is selected to be higher than V_{dc}, which can give L_s a negative voltage to extinguish the fault current in the system.

Different from semiconductor switches in a converter, S_1 normally does not need any high frequency switching actions. Thus, the switching loss is no longer a concern of selecting the main switch for the SSCB. Instead, the key metrics for the semiconductor switch are 1) static on-resistance; 2) saturation current, which needs to be higher than the peak let-through (or fault) current level; and 3) capability to successfully turn off the high fault current.

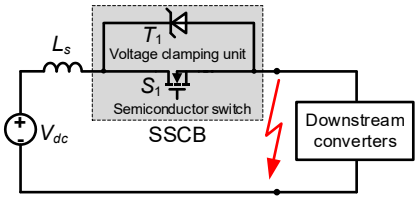

Fig. 1. A SSCB example in a simple dc system.

B. Static Characterization at Room and Cryogenic Temperatures

In this paper, the GaN HEMT GS-065-150 (650 V rated voltage and 150 A rated current @ $T_{SUBSTRATE}$=25°C) from GaN System is selected for the study. The objective is to turn off 500 A (3.3 times of the rated current) using a single bare die at cryogenic temperatures.

The output characteristic of the device is characterized by a curve tracer Keysight B1505A at different temperatures from -180°C to 60°C as shown in Fig. 2. A thermal chamber DELTA9039 is used to control the temperature of the device. The on-resistance of the device is 11.6 mΩ at room temperature (23°C) and is reduced to only 2.6 mΩ at the cryogenic temperature (-180ºC). This low on-resistance is comparable to that of a SiC module with around ten 100 A rated SiC bare dies in parallel [8] while the size is much smaller.

Moreover, in Fig. 2, the saturation current of the GaN HEMT at -180ºC is much higher than that at 23°C. At 23°C, the saturation current starts at around 300 A, while at -180ºC, the device is not saturated yet even when the current is close to 500 A. It was not further tested at higher current conditions because of the current limit of the curve tracer. This high saturation current enables the device to allow a let-through current around or even higher than 500 A, and also provides the prerequisite for 500 A turn-off current during the short circuit protection for the SSCB.

Overall, the GaN HEMT features excellent static characteristics (low on-resistance and high saturation current), making it suitable candidate for SSCBs in future EAP systems.

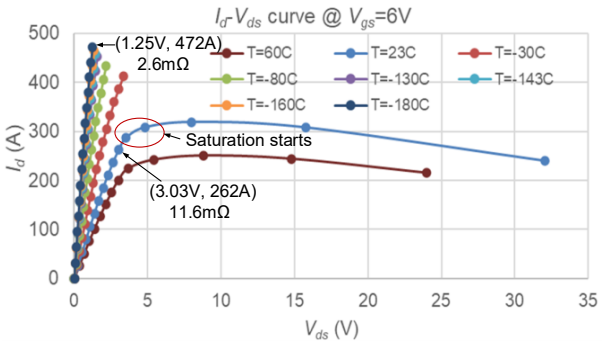

Fig. 2. Static characterization of GS-065-150.

III. High Current Turn-off of GaN HEMT at Cryogenic Temperature: Device Failure and Analysis

The GaN HEMT benefits from the high saturation current, but still needs to be safely turned off at such a high current to qualify for cryogenically cooled SSCB applications. Thus, the dynamic characterization of the device is implemented for the high current turn-off test.

A. Dynamic Characterization for High Current Turn-off

Fig. 3 shows the test platform and associated circuit, which are the same as a regular double pulse tester (DPT). The thermal chamber is also used to control the temperature. For cryogenic temperature, the liquid nitrogen is used as the coolant. The temperature of the liquid nitrogen is around -200°C while the minimum controllable temperature of the thermal chamber is -180°C. The TVS diode AK3-430 from Littlefuse is used as the voltage clamping unit T_1. The GaN HEMT is driven by +6V/-4V and with 20 Ω as both turn-on and turn-off gate resistance R_{g_on} and R_{g_off}. The turn-off current is gradually increased with a step of 20 A to test the device turn-off capability. A high bandwidth (800 MHz) high voltage (1 kV RMS) passive probe TPP0850 from Tektronix is used to measure the drain-to-source voltage of the device, and a Rogowski coil (PEM CWT6B with 1.2 kA AC current measurement range) is used to measure the drain current through the device. The passive voltage probe and the coil part of the Rogowski coil can operate at -180ºC, enabling the test at such conditions. Note that the gate voltage is not measured to avoid the influence on the switching performance.

The turn-off current is gradually increased with a step of 20 A in the pulse tests until it reaches the target turn-off current of 500 A. Fig. 4 shows the drain-to-source voltage v_{ds} and drain current i_d of the GaN HEMT under 440 A, 460 A, and 480 A turn-off conditions at -180°C. The device successfully turned off currents of 440 A and 460 A but then failed at 480 A. The drain current was reduced to a low level (~100 A) during the turn-off, but then suddenly the high frequency ringing of v_{ds} and i_d were observed, and the device falsely turned on. Similar phenomenon and failure turn-off current have been repetitively observed in around 5 different bare dies.

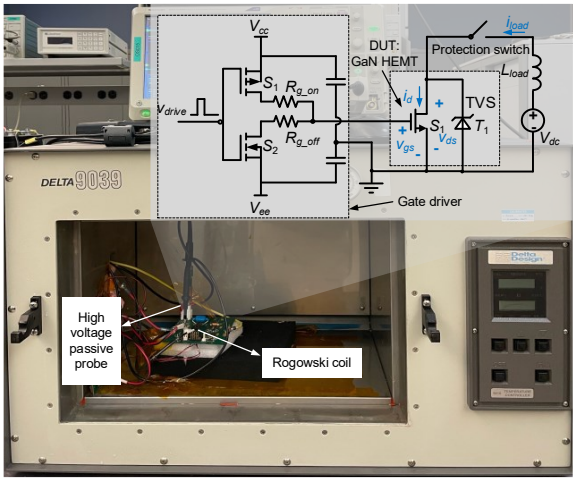

Fig. 3. Test platform of GaN HEMT turn-off capability with a test circuit in it.

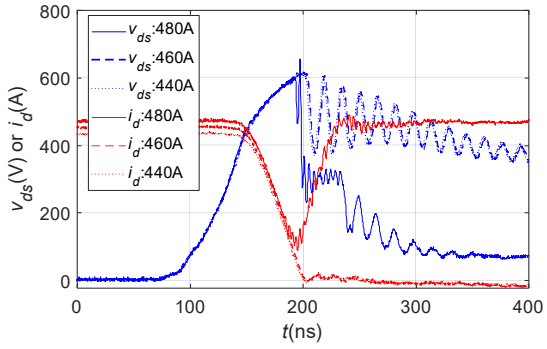

Fig. 4. Test waveforms of GaN HEMT turning off high currents.

B. *High Current Turn-off Failure Analysis*

The potential reason for the failure could be the parallel instability of the multiple switching cells in one GaN bare die. To achieve a high current rating, the GaN die consists of 10 switching cells, as shown in Fig. 5. Each switching cell is equivalent to a 15 A rated bare die GS66504B [9]. These 10 switching cells are paralleled with each other.

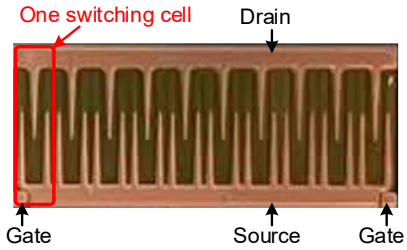

Fig. 5. GaN bare die (GS-065-150) with multiple switching cells.

Based on the analysis from [10], instability can be justified with positive real part of conjugate eigenvalues solved for the state-space model of the paralleling circuit. The equivalent parallel circuit of GaN HEMTs during the turn-off transient is shown in Fig. 6 (a). The parasitic inductances (L_d, L_g, and L_s), and parasitic capacitances (C_{gs}, C_{gd}, and C_{ds}) are considered. Since the device operates mainly in the saturation mode during the turn-off transient, the channel current is modeled as a controlled current source with a current of $g_{fs}(v_{gs}\text{-}V_{th})$. The gate resistance consists of inner gate resistance R_{g_int} and external gate resistance R_{g_ext}. The paralleled equivalent circuit can be decoupled into the common mode (CM) and the differential mode (DM) parts, as shown in Fig. 6 (a). The inner gate resistance R_{g_int} mainly influences the DM part and the external gate resistance R_{g_ext} mainly influences the CM part.

The ringing between paralleled MOSFETs is mainly the DM oscillation based on [11]. Thus, the equivalent circuit can be simplified into Fig. 6 (b). Note only 2 paralleled switching cells are considered in the analysis. For 10 paralleled cells, similar results can be obtained for the stability consideration.

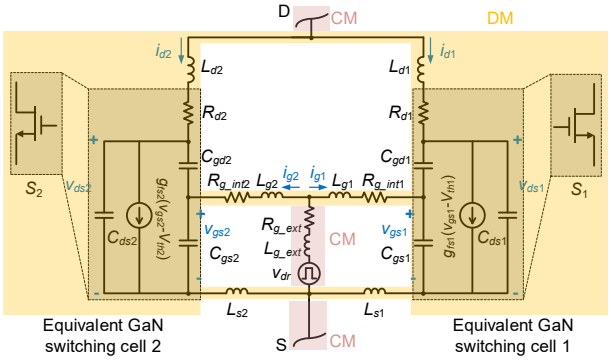

(a) Equivalent circuit of 2 paralleled GaN switching cells.

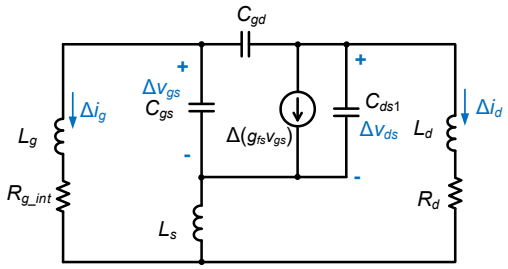

(b) DM equivalent circuit of paralleled GaN switching cells.

Fig. 6. Equivalent circuit of paralleled GaN cells inside the bare die

The general state-space model of the circuit is written as

$$\dot{\vec{x}} = A \cdot \vec{x} \tag{1}$$

where $\vec{x}$ and $\dot{\vec{x}}$ are the state space vector of the circuit and its derivatives, respectively. For the circuit shown in Fig. 6 (b), $\vec{x} = [\Delta i_g, \Delta i_d, \Delta v_{gs}, \Delta v_{ds}]^T$. A is the system matrix, which can be either manually derived or automatically generated with MATLAB and PLECS [12]. In this paper, it is automatically calculated with MATLAB and PLECS.

The eigenvalues λ of the system matrix A can be solved by the equation $|A - \lambda \cdot I| = 0$. Each single eigenvalue λ_i corresponds to a particular solution of the state space variable. The solutions can be expressed as

$$\vec{x}_i = [K_{i1}, K_{i2}, K_{i3}, \cdots, K_{in}]^T \cdot e^{\lambda_i t} \tag{2}$$

where n is the number of state variables and K_{in} is the coefficient determined by initial values of state-space variables. Complex conjugate eigenvalues can be decoupled into the real part α and the imaginary part β. Based on the Euler rule, the solution without the coefficient can be expressed as

$$e^{\lambda t} = e^{(\alpha + i\cdot\beta)\cdot t} = e^{\alpha\cdot t} e^{i\cdot\beta\cdot t}$$
$$= e^{\alpha\cdot t}\cdot(\cos(\beta\cdot t) + i\cdot\sin(\beta\cdot t)) \quad (3)$$

The factor $e^{\alpha\cdot t}$ determines the envelope of the circuit response. For α less than zero, the circuit response is convergent. The more negative the α value, the faster the convergence speed. For α greater than zero, the circuit response is divergent. The greater the α value, the faster the divergence speed.

This analysis is straightforward for a fixed operating point (certain drain-to-source voltage V_{ds} and channel current I_{ch}) or fixed capacitance and transconductance value for the circuit in Fig. 6 (b). However, during the turn-off of the device, the capacitance and transconductance are nonlinear and operating point dependent. The real parts of conjugate eigenvalues are then solved at different operating points (different V_{ds} and channel currents I_{ch}) using the nonlinear capacitance and transconductance curve from the datasheet. Other inductances and resistance parameters are listed in TABLE I. The parasitic inductance is estimated from the size of the bare dies and the distance between switching cells with an empirical rule of 1 nH/mm. The inner gate resistance R_{g_int} is from the gate resistance of GS66504B.

TABLE I. PARASITIC INDUCTANCE AND GATE RESISTANCE USED IN THE MODEL

L_g	L_d	L_s	R_{g_int}
1 nH	1 nH	1 nH	1.4 Ω

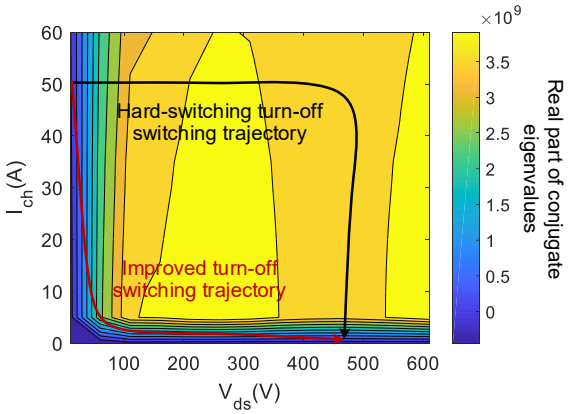

Fig. 7. Stability controur with hard-switching turn-off switching trajectory.

Fig. 7 shows the contour of the solved real parts of 2 paralleled switching cells of the GaN HEMT. There are positive real parts of the paralleled switching cells, which indicates the instability of operating points where the hard-switching trajectory goes through. This unstable region is obvious with V_{ds}>~30 V and I_{ch}>~4 A. The turn-off switching trajectory is also plotted in the contour. With the whole GaN bare die turning off 480 A, each bare die has a turn-off current of 48 A, assuming the current is evenly distributed. The turn-off switching trajectory has most of its part in the unstable region of the stability contour, which could be the reason for the device ringing and failure at a very high current turn-off.

IV. INFLUENCE OF THE VOLTAGE AND CURRENT OVERLAP ON TURN-OFF RINGING AND VERIFICATION

As analyzed in [10], such parallel instability can be improved by altering the turn-off switching trajectory to go through the region with smaller or negative real parts in Fig. 7. These stable regions are normally with either low voltage or low current (e.g., V_{ds}<~30 V or I_{ch}<~4 A). Thus, the improved turn-off trajectory is to decrease the current first at low voltage and then increase the drain-to-source voltage with low channel current. An exemplary switching trajectory is shown in Fig. 7.

A. Using RC Snubber to Minimize Overlap of Voltage and Current during Turn-off

To achieve such an improved turn-off trajectory, in this paper a RC snubber is added across the switch, as shown in Fig. 8. The mechanism is that in the turn-off process, the load current needs to charge the capacitance to increase the drain-to-source voltage. Thus, the channel current keeps low when the drain-to-source voltage increases to reduce the overlap between v_{ds} and i_d.

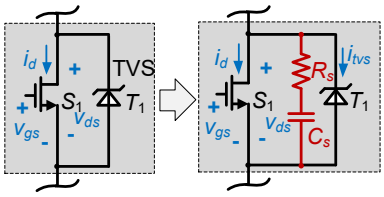

Fig. 8. Add an RC snubber to the SSCB switching cell.

The RC snubber design in the SSCB is different from the one in switching power supplies. In the SSCB, the switching loss is not a concern since no high frequency switching actions exist. Thus, the capacitance C_s can be selected much larger than the output capacitance C_{oss} of the device. However, in switching power supplies, such high extra capacitance can cause very high turn-on loss. The resistance R_s is used here mainly to damp the low frequency ringing between C_s and loop inductance, which is between the switch and the RC snubber. This is similar to the conventional RC snubber. As a result, C_s is selected as 100 nF and R_s is selected as 0.5 Ω. The turn-off switching trajectory with this RC design is shown in Fig. 7. Most of the switching trajectory stays in the stable region with real parts of the conjugate eigenvalues less than zero. Thus, it is possible to use the RC snubber to realize a successful high current turn-off for paralleled switching cells. Note that both R_s and C_s values are not the only solutions, with many other combinations of R_s and C_s also available.

B. Simulation Verification

Simulation is first conducted to verify the instability issue and the effectiveness of the RC snubber. To simplify the circuit, only 3 switching cells (GS66504B) are paralleled and the turn-off current is set as 150 A. The parasitic inductances and inner gate resistance are the same as those listed in TABLE I. The SPICE model of GS66504B from the GaN System website is used, which considers the nonlinear capacitance and transconductance. As seen in Fig. 9 (a), the ringing happens at the external v_{gs}, v_{ds} and i_d when turning off 150 A. With the RC snubber, the switch can turn off successfully without ringing in Fig. 9 (b). The overlap

between v_{ds} and i_d during the switching transient is much reduced when compared to Fig. 9 (a) without the RC snubber.

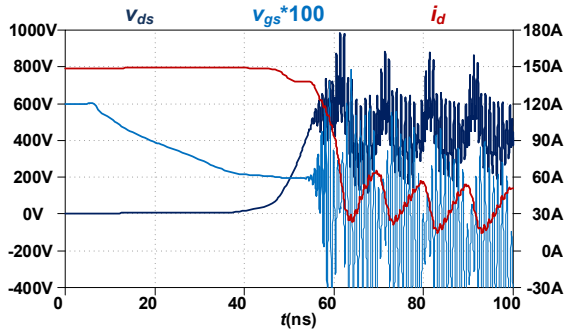

(a) Turn-off instability without RC snubber

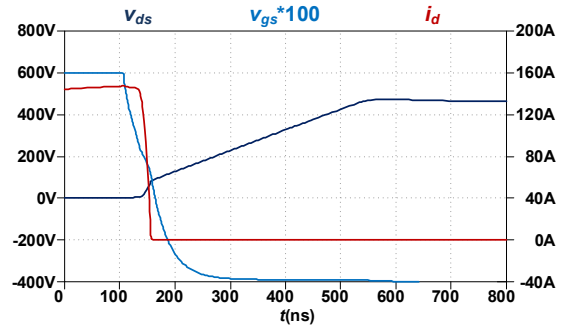

(b) Turn-off with an RC snubber to improve the stability

Fig. 9. Simulation comparison for parallel stability with and without an RC snubber.

C. Experimental Verification

Experiments are conducted through the same setup in Fig. 3. The only difference is the RC snubber is added to alter the turn-off switching trajectory. As shown in Fig. 10, the switch successfully turns off 550 A (10% margin of the objective 500A) with the same gate drive circuit and parameters. During the turn-off, the drain current i_d reduces to zero when v_{ds} keeps low. Only a small overlap between v_{ds} and i_d exists to realize the improved switching trajectory. This verifies the effectiveness of the improved switching trajectory to resolve the instability issue of multiple paralleled switching cells.

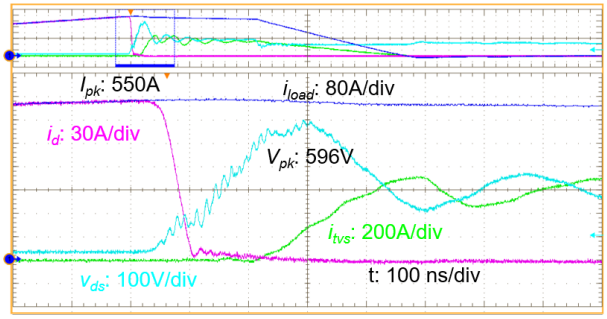

Fig. 10. Successfully turn off 550 A with small v_{ds} and i_d overlap.

V. Conclusions

In this paper, we discussed advantages and challenges of using GaN HEMTs for cryogenically cooled SSCBs. While the on-resistance is reduced to around one-fifth and the saturation current is much increased at cryogenic temperatures compared to the room temperature, the device could have failures during high current turn-off, which could be attributed to the instability of multiple paralleled switching cells in one bare die. The turn-off switching trajectory can influence the stability of the paralleled switching cells based on the analysis of the stability contour of the circuit with various operating points. The turn-off switching trajectory needs be altered to avoid the overlap of high drain-to-source voltage and high channel current. A solution is proposed to use the RC snubber for the high current turn-off. With the proposed solution, the device successfully turns off the 550 A current, in contrast to constant failures around 480 A without the snubber circuit. This test result is consistent with the hypothesis of the instability mechanism.

Acknowledgment

This work is supported by ARPA-e, Department of Energy, USA under the award number DE-AR0001467. This work made use of Engineering Research Center Shared Facilities supported by the Engineering Research Center Program of the National Science Foundation and the Department of Energy under NSF Award Number EEC-1041877 and the CURENT Industry Partnership Program.

References

[1] R. Jansen, C. Bowman, A. Jankovsky, R. Dyson, and J. Felder, "Overview of NASA electrified aircraft propulsion (EAP) research for large subsonic transports," in *53rd AIAA/SAE/ASEE Joint Propulsion Conference*, pp. 4701-4721, 2017.

[2] F. Salucci, C. E. Riboldi, L. Trainelli, A. L. Rolando, and L. Mariani, "A noise estimation procedure for electric and hybrid-electric aircraft," *AIAA Scitech 2021 Forum*, AIAA SciTech Forum: American Institute of Aeronautics and Astronautics, 2021.

[3] P. J. Ansell, "Hydrogen-Electric Aircraft Technologies and Integration: Enabling an environmentally sustainable aviation future," in *IEEE Electrification Magazine*, vol. 10, no. 2, pp. 6-16, June 2022.

[4] F. Wang, R. Chen, and Z. Dong, "Power Electronics: A critical enabler of future hydrogen electric systems for aviation," *IEEE Electrification Magazine,* vol. 10, no. 2, pp. 57-68, 2022.

[5] R. Chen and F. F. Wang, "SiC and GaN devices with cryogenic cooling," *IEEE Open Journal of Power Electronics,* vol. 2, pp. 315-326, 2021.

[6] AS4805-General standard for SSPC, SAE Aerospace Standard, 2007.

[7] R. Ren, H. Gui, Z. Zhang, R. Chen, J. Niu, F. Wang, L. M. Tolbert, D. Costinett, B. J. Blalock, and B. B. Choi, "Characterization and Failure Analysis of 650-V Enhancement-Mode GaN HEMT for Cryogenically Cooled Power Electronics," *IEEE Trans. Emerg. Sel. Topics Power Electron.,* vol. 8, no. 1, pp. 66-76, 2020.

[8] J. Hayes, K. George, P. Killeen, B. McPherson, K. J. Olejniczak, and T. R. McNutt, "Bidirectional, SiC module-based solid-state circuit breakers for 270 V dc MEA/AEA systems," in *2016 IEEE 4th Workshop on Wide Bandgap Power Devices and Applications (WiPDA)*, pp. 70-77.

[9] GaN System Datasheet GS66504B, [Online]. Available: https://gansystems.com/wp-content/uploads/2020/04/GS66504B-DS-Rev-200402.pdf

[10] Z. Dong, R. Ren, W. Zhang, F. F. Wang, and L. M. Tolbert, "Instability Issue of Paralleled Dies in an SiC Power Module in Solid-State Circuit Breaker Applications," *IEEE Trans. on Power Electron.,* vol. 36, no. 10, pp. 11763-11773, 2021.

[11] J. G. Kassakian and D. Lau, "An analysis and experimental verification of parasitic oscillations in parralleled power MOSFET's," *IEEE Transactions on Electron Devices,* vol. 31, no. 7, pp. 959-963, 1984.

[12] UTK ECE692 Material, [Online]. Available: http://web.eecs.utk.edu/~dcostine/ECE692/Fall2019/tutorials.php?topic=PLECS